# Mineralogical and chemical characterization of Bottom Ashes from Municipal Solid Waste Incinerator

*A multi-techniques approach for an extremely complex and heterogeneous material*

**Chiara De Matteis**

Dipartimento di Scienze Chimiche, della Vita e della Sostenibilità Ambientale, Università di Parma, Parco Area delle Scienze 157/A, 43124, Parma, Italia

DOI:10.19276/plinius.2023.01.006

## INTRODUCTION

Humanity is now a dominant geological actor, as human activities induce great, multiple and irreversible changes on Earth. The study of these human-associated changes led to the suggestion that we should not refer to the present time as pertaining to the Holocene epoch but to a new geological epoch called the "*Anthropocene*" (Crutzen, 2002; Steffen, 2021; Trischler, 2016; Zalasiewicz et al., 2011). This new epoch is characterized by the appearance of "*new materials*": a set of anthropogenic materials, which do not exist in nature, designed by man through the development of research and technology and born to satisfy the needs of our society. An important input of anthropic material in environmental matrices is given by the production of waste.

The EU policy strategy for waste reduction and management is based on the following principles, in order of preference: prevention, reuse, recycling, recovery and disposal. A *recovery* strategy is to send Municipal Solid Waste (MSW) to Waste-to-Energy (WtE) plants, that reduce mass and volume of input waste up to 25% and recover energy from waste in the form of heat and electricity (Brunner & Rechberger, 2015). From the combustion of waste not only energy is obtained but also residual ashes.

BA are one of the major by-products obtained during MSW incineration in WtE plants; their mass is about 20% of the incinerated waste. Once the incineration process is complete, the BA are thrown into a tank full of water for rapid cooling. The BA are classified as non-hazardous waste (EWC code 19.01.12: bottom ash and slag other than those in 19.01.11 *).

The BA are very heterogenous materials made up of different fractions (glass, synthetic ceramic, mineral, metals and unburning organic matter) which, thanks to the non-hazardousness nature of the unburned material, can be recycled becoming a resource. The mineralogical and chemical composition of BA varies due to the different waste input, combustion temperature, plant type, quenching, aging and weathering.

The most common mineralogical phases are (i) silicates (quartz, melilites, feldspars), (ii) carbonates (calcite, vaterite), (iii) oxides (magnetite, hematite, corundum), and (iiii) hydrated phases typical of cementitious materials (hydrocalumite, portlandite, ettringite, stratlingite). In addition to these main phases, a high content of amorphous material, is also present (Alam et al., 2019; Bayuseno and Schmahl, 2010; Bertolini et al., 2004; Caviglia et al., 2019; Mantovani et al., 2023).

Chemically, most abundant elements in BA such as Al, Fe, Si, Ti, K and Na are very close to those of the continental crust. Among the minor and trace elements, Co, Zr, Li, Hf, Ti, Rb, F, V, Mn, Sr, Ga, U, Th show an average composition in BA similar to the earth continental crust content, whereas a significant enrichment in BA is found for Cl, Zn, Cu, S, Pb, Br, Mo and Sn. The presence of these *Potential Toxic Elements* (PTE) poses an issue about the potential toxicity of the BA. The toxicity of an element depends on its oxidation state and/or its concentration in a given environment, which depends on its leachability. On its turn, the leachability of an element in environmental matrices depends on the mineralogical phase in which it is hosted. Investigate the chemical form of PTE and know the crystalline and amorphous phases that host them is a key point in assessing the potential toxicity of BA and to implement safer and viable material recycling strategies.

This complex chemical and mineralogical composition and the presence of PTE gives rise to numerous scientific questions regarding their reuse and non-hazardousness. In this work a multi-techniques approach was used to characterise BA and understand the distribution and behaviour of PTE.

## MATERIALS AND METHODS

### Sampling and sample preparation

The BA studied in this work were sampled from 5 WtE plants in different cities of northern Italy: Parma (PR), Piacenza (PC), Torino (TO) (plants owned by the company *Iren Ambiente*), Ferrara (FE) and Forlì-Cesena (FC) (plan-

ts owned by the company *Hera Ambiente*). Forlì-Cesena WtE plant burns only MSW while the others burn special non-hazardous waste. The BA investigated were taken randomly from a 2-3 m high stock, representative of more than one month of accumulation. Approximately 5 kg of BA samples were collected from each plant.

### Grain size analysis

The samples from the 5 WtE plants were first dried in an oven at 50°C for 24h and then sieved into ten grain size classes (Φ : 16, 8, 4, 2, 1. 0.5, 0.3, 0.2 e 0.063mm) according to the prescriptions of the European standards for aggregates EN 933-2 (Ente Nazionale di Unificazione, 2020).

Each particle size class was weighed and, by calculating the percentage of material that passed through the sieves, cumulative particle size curves were made in order to evaluate their distribution and mechanical qualities.

### Thermo Gravimetric Analysis (TGA)

TGA were conducted on samples taken from each particle size class by a Perkin Elmer 8000 instrument equipped with a Pt-crucible at a heating rate of 10 °C/min in the temperature range 35°C – 800 °C. All the measurements were run under a constant flux of dry air atmosphere (30 mL/min).

### SEM – EDS observations and analysis

As a preliminary step, several grains (8 - 16 mm) were observed with a Scanning Electron Microscope coupled with Energy Dispersive System (SEM-EDS) JSM IT300LV Jeol 6400 equipped with an Oxford EDX microprobe. Microprobe analysis was performed with operating conditions 20 or 25 kV and 1.2 mA current, ~1μm beam diameter and 75 s counting time.

Subsequently, a great quantity of granules (0.5 – 1 mm), were embedded in epoxy resin stabs, cut longitudinally and analysed by a JEOL JSM-IT 300LV Scanning Electron Microscope, equipped with Oxford INCA Energy 200 EDS SATW detector (WD 10, KV 15), at 15 kV, 1.2 mA current and 1μm beam diameter.

### X – Ray Powder Diffraction (XRPD) Analysis

For each grain size, XRPD was used for the identification and quantification of the phases in the samples using a Bragg-Brentano Bruker 2D Phaser Diffractometer, with θ – θ geometry, Cu Kα radiation, 30 kV and 10mA and a solid-state detector.

Quantitative analysis was done by means of the Rietveld method.

### X – Ray Fluorescence (XRF) Analysis

#### *XRF spectroscopy: conventional source*

Chemical composition was analysed for each grain size with a WDXRF Axios PanAlytical spectrometer, equipped with a Rh tube working at 4 kW. The analyses were performed on both major elements (expressed g/100g) and trace elements (expressed in g/Kg).

#### μ - *XRF spectroscopy: synchrotron radiation*

μ - XRF maps were done at the XRF beamline at Elettra Sincrotrone Trieste (ETS). The experiment has been conducted using both HE multilayer for the collection of μ-XRF maps, with standard 45°/45° geometry for fluorescence mode measurements, using an XFlash 5030 SDD detector (Bruker, Berlin, Germany). μ-XRF maps were collected with an incident beam energy of 14 keV and a beam size at the exit slits of 50x50 $\mu m^2$ (H*V).

### X-ray Absorption Near Edge Structure (XANES)

Some PTE (Cu, Cr, Zn, Pb, Ni, and Co) were analysed by XANES in order to investigate their oxidation state and the mineralogical environment in which they were hosted. XANES measurements were conducted at the XRF beamline at Elettra Sincrotrone Trieste (EST). The experiment has been conducted using Si111 monochromators, with standard 45°/45° geometry for fluorescence mode measurements, using an X-Flash 5030 SDD detector (Bruker, Berlin, Germany). All spectra were collected using 5 seconds per step and a variable energy step as a function of the energy: Large step (5 eV) in the first 200 eV of the spectrum, smaller step (0.2 eV) in the near-edge region and a k-constant step of 0.05 Å-1 further above the absorption edge. The oxidation state will be determined using least-squares Linear Combination Fitting (LCF) based on reference spectra collected on compounds of known oxidation state.

### Leaching Test

Leaching tests and analysis of the leachates were performed following the *UNI EN 12457-2:2004 "Waste Characterization - Leaching - Compliance test for granular waste and sludge leaching - Part 2: Single-stage test with a liquid/solid ratio of 10 l/kg for materials with particle sizes less than 4 mm (with or without size reduction)"*. The test was carried out on the particle size classes below 4 mm from all the five WtE plants examined.

Eluates collected were analysed by: *Atomic Absorbition Spectroscopy (AAS)* (Thermo S Series AA Spectrometer) for cations (Ca, Mg, Na, K); *Ion Chromatography (IC)* (Metrohm Compact IC pro 881) for anions ($Cl^-$, $SO_4^{-2}$, $F^-$, $Br^-$, $PO_4^{3-}$); *Inductively Coupled Plasma – Mass Spectrometry (ICP - MS)* (Perkin Elmer ICP-MS ELAN DRC-e) for the investigation of trace elements (Al, Ba, B, Cr, Co, Fe, Pb, Li, Mn, Mo, Ni, Se, Sr, Tl, Ti, V, Zn).

### Sequential Extraction Procedure (SEP)

A new 5 - step SEP was set in this work. SEP was performed on BA (0.063 – 0.2 mm, 0.3 – 0.5 mm, 2 – 4mm and < 4 mm) sampling from Parma WtE plant.

Solid residues obtained from each step were analysed by XRPD and XRF.

Eluates collected were analysed by Agilent 7500 ICP-MS for the investigation of critical raw elements.

Statistical analysis

The results obtained were investigated by statistical analysis using: *Pearson's r index (r-index)*, *correlation index R (or p) by Spearman ranks* and *Principal Component Analysis*.

## RESULTS AND DISCUSSION

### Bottom Ashes morphology and composition

Optical observation was done on several grains, chosen for different colour and lustre, from the portion larger than 4 mm. The grain colour varies with the crystalline and amorphous phase content, as revealed subsequently by XRPD. The rounded reddish-grey grains, which are most abundant, are mainly made by a heterogeneous aggregation of residual refractory material and metals coexisting with crystals and amorphous (Fig. 1d). The amorphous acts as a matrix that binds the crystalline and metallic fractions (Fig. 1b) of the original waste and the new-formed minerals. The original waste grains show rounded edges, indicating partial reabsorption (Fig. 1c), whereas new formed crystals are often present as sharp needles within the glass. Vesicles and bubbles appear indicating that some degassing occurred (Fig. 1a).

The bulk mineralogical composition for each WtE plant was obtained from each grain size. The main mineralogical phases are reported in Table 1 whose abundance has been refined by Rietveld analysis. A number of minor phases is also present, which either showed very faint peaks in XRPD. During Rietveld analysis it was shown that the inclusion of a higher number of phases leads to refinement instability, so that a compromise was necessary between the number of phases to be included and the number that could be refined. Most evident is the amorphous content, which is higher in the BA of the three plants (TO, PR, PC) so as that it overtakes the entire quantitative of crystalline component. In these plants, the amorphous is over 75% on average, and ranges in different grain size between 67 and 88 wt%. In the plants of FE and FC, instead, bulk amorphous is, on average, less than 35% (depending on grain size between 7 and 55 wt%). The lower quantity of amorphous material in FE and FC occurs together with higher calcite, quartz and feldspar. Also, ettringite content is higher in FE and FC than the other 3 plants sampled, indicating a probable greater reactivity of these ashes in the aging process.

Among minerals, quartz, calcite, melilites, iron oxides and some alteration products such as sulphates, chlorides, and hydrated minerals are ubiquitous. Strätlingite is found only in the PR samples. This mineral is typical of cementitious materials and can be formed either from the degradation of gehlenite or from the reaction between calcium silicates ($Ca_2SiO_4$- belite) with $Al(OH)_3$ in hydration processes involve the degradation of gehlenite, as some evidence found in SEM analyses showing that gehlenite has been formed in the combustion chamber (crystals with typical neoformation and rapid cooling shape). Iron-containing minerals as hematite and magnetite are revealed by X-ray diffraction, although likely other metal phases are present like Cu or Ni-Ti alloys. Last, a number of silicate phases, like pyroxene, gehlenite-akermanite, and anorthite, are found without significant difference with grain size, and are likely formed at high temperature in the combustion chamber.

According with XRPD data, the bulk chemical composition of BA is represented by the major oxides of Si, Ca, Fe and Al. In fact, the sum of these elements (in oxides) represents from 60 to 77 g/100 g. S and Cl are found in

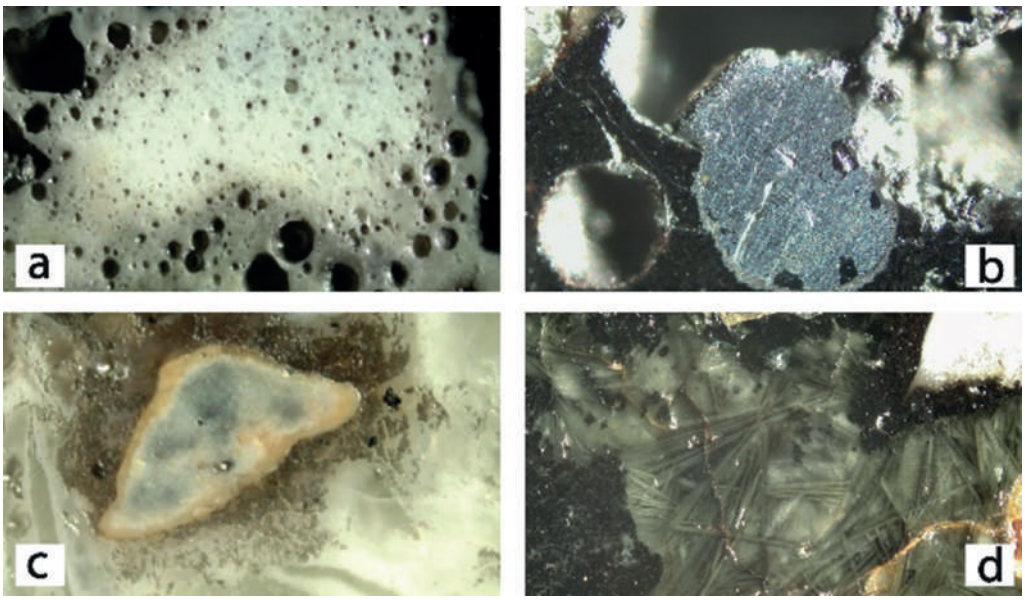


***Figure 1*** *Photomicrograph showing the inner part of the clasts cut longitudinally. Each of them appears different from the other in terms of morphology but we can observe frequently a part of a dark matrix (b,d) and within it areas of different color, sometimes white (c) or transparent (d). Many samples present little vesicles and bubble structures, indicating degassing processing (a), metallic, alloy or refractory inclusions (b) sometime with reaction rims (c).*

*Table 1 XRPD identification of bottom ash. The minerals are arranged in the following sequence: (x) major minerals (*) minor or trace minerals, (/) not found or very doubtful presence.*

| Mineral phase | PR | TO | PC | FE | FC |
|---|---|---|---|---|---|
| calcite | X | X | X | X | X |
| vaterite | X | X | X | X | X |
| quartz | X | X | X | X | X |
| cristobalite | / | / | * | / | / |
| plagioclase | X | X | X | X | X |
| pyroxene | * | * | * | / | / |
| melilite | X | X | X | X | X |
| ettringite | X | X | X | X | X |
| hydrocalumite | X | X | X | X | X |
| portlandite | X | X | X | X | X |
| strätlingite | X | * | * | * | * |
| apatite | * | * | * | * | * |
| larnite | * | * | * | x | x |
| tobermorite | * | * | * | / | / |
| sjogrenite | / | / | / | * | * |
| magnetite | X | X | X | X | X |
| hematite | X | X | X | X | X |

a range from 0.3 to 2 g/100g. Among minor elements, Zn, Cu, Pb and Ba content is higher than 1000 mg/kg. The oxides show a rather similar pattern in the different plants, albeit with some slight difference: the BA from TO show higher $Fe_2O_3$ and lower CaO, and those from PC shows lower $SiO_2$ and higher LOI than the others. Also, for minor and trace elements our data show that the compositional variability related to grain size. In PC higher value are found for Cl, and Cu, and overall, a higher compositional spread in S, Cl and Zn content. The smaller fraction is richer in Ca due to the faster carbonation occurring in smaller particles with larger surface area. Si is positively correlating with grain size probably due to the glass shards in larger grain size. Na as well correlates with Si, possibly for the addition of Na as a fining agent in glass production technology and for the presence of plagioclase solid solution. Ca, Ti, S, LOI (in all the plants) and Cl (in PR, PC, FE) correlate negatively with grain size. The higher Ca in smaller particles goes together with the higher Ca-carbonate content. Higher decarbonation means also higher weigh loss in LOI, which is greater in smaller particle sizes having higher active surfaces. We suppose that S follows the same trend due to the sulfation process and the formation of the ettringite phase, which, as shown in XRPD analysis, is more present in finer sized grains. Most of the PTE like Cu, Pb and Cr are negatively related with grain size. To note, the differences in the minor elements concentration between plants could be related to the different waste input. Other elements, like Al, Fe, Mg, P and Cr show little change between samples of different grain size. An exception in TO is MgO and $Al_2O_3$, which show a significant increase in the smaller sized grains. S and Cl are contained in the BA in considerable quantities, causing metal erosion if they are used as supplementary cementitious material in reinforced concrete. In BA examined in this work, S and Cl range between 2000 to 21000 mg/kg. These two elements are positive correlated in all incinerators and show an inverse correlation with the grain size, suggesting that they are mostly present as weathering of the products.

TGA shows a continuously weight decreases with temperature for any grain size. The weight loss is higher in the smaller grain size, where the mass loss at 800°C is about 25%. For the larger grain size, the loss is about 5-10% and for intermediate ones about 15%. An exception is PC, where the weight loss is similar for every grain size. The analysis of the first derivative shows few temperature ranges where higher weigh loss is present. A moderate (3-4%) weight loss occurs in the interval 50-100°C, likely ascribable to two reaction: one at 50-60°, likely due to surface water, and another just above 100°C, related to the first dehydration of ettringite with further dehydration possibly revealed by the faint peaks at 250 and 350°C. The second loss is 1-2 wt% and appeared over the range 250-450°C and a 4-7 wt% in the interval 620-760°C. The 250-450°C reaction is likely due to plastic combustion residue (molecular decomposition), while the 620-760°C loss is ascribable to the transformations involving carbonate (decarbonation) phases. In FE and FC the de-carbonation loss is greater than in the other plants, accordingly with XRPD and XRF data that show a higher carbonate content. Despite the general shape of the TGA curves appear similar, some difference with particle size dimension and between plants is found. A peak at 450°C has been found only in FE and FC BA. The peak is more apparent in the finer portion, and it is likely due to the de-hydration of portlandite which occurs between 450 and 500°C. Portlandite is present only in the two incinerators of FE and FC, between 5-10 wt% in the finer portion, and between 1 and 2% in the larger grains.

Potential Toxic Elements speciation and behaviour

Prediction of leaching behaviour in a complex system like BA involves the phases within the ashes, their proportion, and their thermodynamic properties in multiple equilibria. For these reasons, PTE behaviour must be study by a multi-technical approach.

XANES analyses together with a μ-XRF mapping by synchrotron radiation and SEM - EDS allowed to investi-

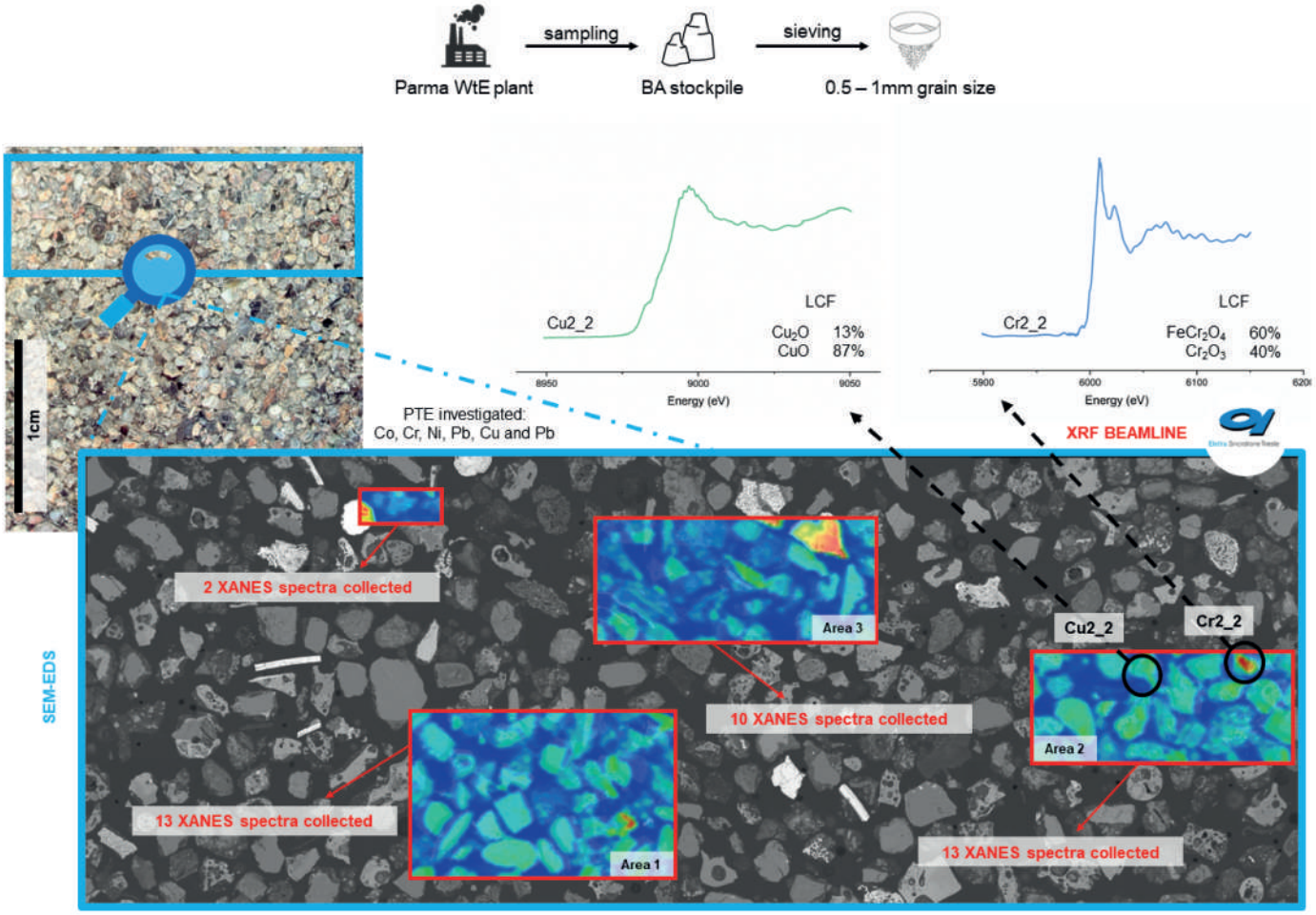


*Figure 2* Graphical abstract of the experiment conducted at the Elettra XRF beamline, Sincrotrone Trieste.

gate distribution and speciation of PTE (Fig. 2). XANES spectra collected at the Cu K-edge in different clasts suggests that Cu chemical environment and oxidation state are heterogeneous even in the same area (0, +I and +II); this is interpreted as an effect of zones in the fuel bed with different access to the oxygen. Pb is present in +II and +III chemical forms. In all XANES spectra Cr was present in the Cr 0 and Cr III+ oxidation state. No evidence of Cr VI+. Zn was found in BA in a number of different phases, some of them well visible also in SEM-EDS. Various XANES spectra were collected on different clasts. Zn is not present as a metal but mainly occurred in oxidation state +II. In all the spectra, a great fit is obtained with Zn-carbonate, in the form of smithsonite ($ZnCO_3$) or hydrozincite ($Zn_5(CO_3)_2(OH)_6$). Zincite (ZnO) was found in few grains, confirming SEM-EDS results. Also, spinel phases like gahnite and Zn-ferrite ($ZnFe_2O_4$) are present, as well as the silicate hemimorphite [$Zn_4Si_2O_7(OH)_2 \cdot H_2O$]. Ni is found in SEM-EDS only in the above described grain together with Co. Ni is present in metal and oxidized form, but hydration is also possible.

Leaching tests were done on particle sizes below 2 mm, as XRF analyses showed that they are richer in PTE. Marked differences in leaching behaviour have been found between the two different owner corporation that is IREN for PR, PC and TO and HERA for FC and FE. With respect to a given particle size, the leaching of an element has been compared to the total content in the bulk sample (from XRF analysis) and calculated in percentage (all referred to mg/kg of material). The most released element is Cl with a release percentage of about 70/90%, higher in the finer fraction. We suggest that Cl is present in very soluble salts, like NaCl and KCl, dispersed on the surface of the grains. This suggestion is confirmed by the linear relation found in leached Na+K with Cl, whereas such relation does not exist in the sample composition determined by XRF as most Na and K are likely caged within the amorphous and silicates structures. Therefore, no diffraction peaks attributable to Na, KCl are found in XRPD analysis, suggesting that not all the Cl is bound to Na and K in salts, and that a significant release of Cl may be originate by the dissolution of ettringite. SEM - EDS analyses of the ashes showed that Cl is often associated with silicate glassy phases. We suggest therefore that chloride is most released by dissolution of weakly bonded Cl at the surface of the amorphous phases. All tests exceeded the legal limits for Cl (Legislative Decree 152/06) suggesting that washing and selection of larger grains may be combined technique to reduce Cl for a correct reuse. S shows a release, about 30% for PR, PC and TO and 3% for FE and FC, with no dependence on the particle size. S is present in the ettringite structure which is observed in XRPD in all the plants, especially in FE and FC. However, the release in $SO_4^{2-}$ is lower in the

two HERA WtE plants, whereas the Ca is higher. Moreover, Al is released by at least two order of magnitude less in HERA than in IREN plants. Another relevant difference is that the measured pH in the leached IREN plants is between 10 and 11, whereas in the HERA plants it varies between 12 and 12.5.We suggest that in the HERA plants, the dissolution of portlandite, which is absent in the IREN plants, gives rise to a basic environment, where ettringite is less prone to dissolution. In the IREN plants, ettringite dissolves, with sulphate and Al hydroxide solubilization. Therefore, probably the contribution of ettringite dissolution is minor, due to the very similar ratio in Na+K/Cl in the 5 plants, in spite of the different amount and solubilization of ettringite. The different mineralogy in IREN and HERA plants, and the consequent different leaching in major elements has an effect also on minor elements. Minor elements are often present in solid solution within phases more or less prone to dissolution at different pH, and the dissolution of the host phases releases also the exsolved element. Therefore, the release in minor elements is different in the different WtE plants, often by two order of magnitude. For instance, sulphate and Cr are above regulatory limits only in IREN BA, but Ba and Ni (with the exception of TO) only in the HERA plants. A likely interpretation is that Cr could have a significant concentration in ettringite, which is dissolved in IREN plants, whereas Ba and Ni could exchange with Ca in significant amount in portlandite, which is dissolver in HERA plants. In TO the leaching of $SO_4^{2-}$, Co, Cu and Zn is higher than in other plants. Cu, Cr and Ni are, among the PTE, the most released in all plants with values below 0.5%, except for TO where the Cu stands at 3%. On the other hand, the release of Ti, Pb and Zn is relatively low (<0.01%), never exceeds law limits (Legislative Decree 152/06) suggesting their presence in a non-soluble structure, like glass or silicate minerals.

The SEP has been specifically adapted for BA. Some steps have been added and/or modified compared to the BCR standard method up to obtain a five-step extraction procedure to remove i) water-soluble phases, ii) carbonate phases, iii) reducible fraction, iiii) oxidable fraction and iiiii) residues. The leaching of a few elements (Pb, Cu, Zn, Mn, Ni, Fe, Cr and Ti) was investigated by ICP-MS analysis after each step. As expectable they have different behaviour, for they are hosted in different mineralogical and/or amorphous environments. Due to the heterogeneity of BA, it is difficult to create a link between the element and the hosting phase: The element may be present as an impurity or as a major constituent of a given phase. In the latter case such phases are present in a concentration below 1% and are not detected by XRPD. This could explain the high release of some elements, such as Pb and Zn, even if no mineralogical phase having these elements was identified by XRPD. Yet, some speculation can be done by the results of the ICP-MS analyses of the leachates. In the first step, some release was recorded for Fe and Cu, although in a small proportion. Cu could possibly be hosted in chloride, and Fe in larnite, both as impurities. The almost negligible extraction suggests that these elements are not present in salts or water-soluble phases. In second step, Pb and Zn are most leached, showing both a weight loss between 50 to 70% of their original budget. Almost all of the leached Zn was extracted in this step, recording a release of about 70% in both grain size. XANES analysis found Zn typically associated to carbonates, like smithsonite ($ZnCO_3$) or hydrozincite ($Zn_5(CO_3)_2(OH)_6$), or to hydroxides like $Zn(OH)_2$, which are leached by acid attack. For Pb, the leached fraction ranges between 47 and 64% in larger and smaller grains, respectively. XANES analysis showed that Pb could be present as a carbonate and as $Pb_3O_4$, both phases unstable in a highly acid environment. Also, other oxide phases found in SEM-EDS analysis of the BA, like $Ca_2PbO_4$, are soluble in acid environment. Cu present a moderate release at this step, about 35% for < 4 mm and 22% for 0.3 – 0.5 mm grain size. Its presence can be inferred as a carbonate phase and within amorphous phases that are removed in this step. In the third step, the most released elements are Ni, with a percentage in leachates of about 22% in the < 4mm grain size and 14% in the 0.3 - 0.5 mm grain size, Ba and Pb, both with a release of about 10%. At this stage Fe/Mn oxyhydroxides dissolution was rather small, testified by the small weight loss in Fe and Mn. In fourthy step, Ni and Cu are the elements most leached. For Cu it is about 50% of the bulk composition. SEM-EDS and XANES showed for both elements that they are commonly found as metal droplets within a silicate matrix, which are oxidized in a soluble ionic species. Other elements are most concentrated in the residuals: Cr, Fe, Mn and Ti may be present in silicate glass or in spinel oxides; Ba could likely occur as an impurity in feldspars.

## CONCLUSION

The mineralogy, chemical composition and properties of the BA in five WtE plants in Northern Italy were examined. The average composition, and the changes of the composition with grain size follow quite similar trends in all the incinerators. The major and minor elements compositions are very similar, and are well grouped in the compositional variation of the incinerators worldwide. This may indicate that, in spite of the different type of input waste, the chemical output is comparable, at least in the residual fraction. On the other side, there are orders of magnitude in the leached fraction between the different WtE plants, with higher differences between the plants of FE and FC, and the others. The difference is related to the mineralogical composition i.e where a given element occurs in a more soluble phase, and affects also whether the ashes are beyond legislation limits.

The quantitative mineralogical differences (amorphous, carbonates) found between the WtE plants of IREN and HERA groups could be related to some different local burning temperatures, operating procedures or weathering conditions, and make an example on how the mineralogy may affect the properties of the ashes. The combined SEM-EDS, XRF-XANES, XRPD analyses on different grain size and different grains enabled to find a number of new mineral hosts of the PTE (Co, Zn, Ni, Cu, Pb, Cr), found in metallic inclusions, oxides, carbonates, and amorphous matrices. As a combined investigation was not yet previously done, we may assume that the mineralogical variety which has since now been determined in BA, already represented by a considerable number of phases, is just a fraction of the actual one. As long as SEM-EDS is used on single grains, we observe that each grain shows chemically different bulk composition, and mineralogical assemblages. Just for an example Zn was found in BA in 27 mineral phases, of which 15 were confirmed or discovered in this work. Also, what is generally and simply described as an amorphous or glassy phase, is in fact a number of different phases, each of them in local equilibrium with the embedded crystals. This makes the prediction of the leaching behaviour of the ashes a risky task: the leached fraction for PTE is just a very small fraction, between 10-3 and 10-6 of the global content of the element, and a slight change in mineralogy, hardly or not detectable by XRD, may have a profound effect on the leaching of the samples. The precipitation of a small amount of a highly soluble phase containing PTE may increase dramatically the leached fraction.

There are however some regular features in the compositional relations between the elements, which could be outlined by the analysis of different portions of the same sample, sorted by grain size. Two opposite trends are observed: one shown by Si and grain size, the other, opposite correlated to the first, is shown by Ca, Cl, S and the residual loss on ignition. The first trend is followed also by some more lithophile elements, like Zr and Rb, the latter likely present in feldspar or silicate glass. The second trend is followed by PTE elements like Cu and Zn, but with some exceptions: in the BA from PC Zn does not follow a specific trend, and in the FC plant, Cu follows the Si trend. Pb, Ni and Cr do not follow neither trend, with the exception of the FE plant, where Pb goes with S. It appears that Cu and Zn are hosted in carbonate, sulphate or chlorides in the different grain size, whereas Pb, Ni, Co and Cr may have different host minerals in the different compositions. As for the leaching behaviour it is generally observed that leaching increases as the grain size decreases, for Cl , Na (and K) and Cu, but other elements, like Cr and Ni follow a different trend in the WtE plants of TO, PC and PR, where they follow the trend of Cl and Na, respect to FE and FC, where they seem unrelated to the grain size. This again, highlights the difference between the different plants.

For a possible recycle of the BA, the results in leaching tests indicate that all the grain size below 2 mm, from any WtE plants are beyond legal limits for some element. Cl and Cu are always beyond legal limits, and again we find a difference between WtE plants: Ba, Ni, F are above limits in the FE and FC plants, $SO_4^{2-}$ and Cr for the other incinerators. Ni and other elements, like Pb and Zn were always leached below limits, although in FE the Pb leaching is close to the critical value. Therefore, to make any use other than as insulator fillers, some kind of treatment is needed. The observation that PTE decrease with increasing grain size, is not always correct, and for Cu and Cl, in the examined grain size the leaching is so high that it is not expectable that simply sieving the larger portion will solve the issue. However, the larger grain size could be easier to wash, and the reactivity in the grains could be slower: our SEP showed that the leached fraction, no matter its toxicity, is higher in finer grains. The highly reactive nature of the ashes can be used as an aggregate in cement, most for highly maturated material where cement minerals are present. Concrete obtained using BA as aggregate could fix the PTE in a structure where leaching occurs less. By this respect an investigation on the performance and on the leaching of concrete, obtained using ashes of different grain size as aggregates in concrete, before and after washing could be promising. Also, in light of the observed differences in the mineralogy of the different incinerators, we may expect different performances in concrete using ashes from different plants. Preliminary washing at some pH value should be useful, as our observation showed that most of the coarser grains do show a rim, made by smaller grains, and likely the more reactive part. The washing should be made as to disaggregate the rim portion, whose sewage could be subject of further recovery of metals.

## REFERENCES

Alam, Q., Schollbach, K., van Hoek, C., van der Laan, S., de Wolf, & T., & Brouwers, H.J.H. (2019): In-depth mineralogical quantification of MSWI bottom ash phases and their association with potentially toxic elements, *Waste Manag*, **87**, 1–12.

Bayuseno, A.P., & Schmahl, W.W. (2010): Understanding the chemical and mineralogical properties of the inorganic portion of MSWI bottom ash, *Waste Manag*, **30**, 1509–1520.

Bertolini, L., Carsana, M., Cassago, D., Curzio, A.Q., & Collepardi, M. (2004): MSWI ashes as mineral additions in concrete. *Cem. Concr. Res*, **34**, 1899–1906.

Brunner, P.H., & Rechberger, H. (2015): Waste to energy - key element for sustainable waste management, *Waste Manag*, **37**, 3–12.

Caviglia, C., Confalonieri, G., Corazzari, I., Destefanis, E., Mandrone, G., Pastero, L., Boero, R., & Pavese, A.

(2019): Effects of particle size on properties and thermal inertization of bottom ashes (MSW of Turin's incinerator), *Waste Manag*, **84**, 340–354.

Crutzen, P.J. (2002): The "anthropocene", *J. Phys. Arch. IV Fr,* **12**, 1–5.

Ente Nazionale di Unificazione, E.N.I. (2020): Tests to Determine the Geometric Characteristics of Aggregates – Part 2: Determination of the Particle Size Distribution – Control Sieves, Nominal Dimensions of the Openings, UNI EN 933-2: 2020. Milan.

Mantovani, L., De Matteis, C., Tribaudino, M., Boschetti, T., Funari, V., Dinelli, E., Toller, S., & Pelagatti, P. (2023): Grain size and mineralogical constraints on leaching in the bottom ashes from municipal solid waste incineration: a comparison of five plants in northern Italy, *Front. Environ. Sci*, **11**, 1–15.

Steffen, W. (2021): Introducing the Anthropocene: The human epoch. *Ambio*, **50**, 1784–1787.

Trischler, H. (2016): The Anthropocene: A Challenge for the History of Science, Technology, and the Environment. *NTM Int. J. Hist. Ethics Nat. Sci. Technol. Med*, **24**, 309–335.

UNI EN 12457-4 (2004): Waste characterization–leaching–compliance test for leaching of granular and sludge waste–Part 2: Single stage test, with a liquid/solid ratio of 10 L/kg, for materials with particles smaller than 4 mm (with or without size reduction). Available at: https://store.uni.com/en/uni-en-12457-4-2004 (Accessed October, 2021).

Zalasiewicz, J., Williams, M., Fortey, R., Smith, A., Barry, T.L., Coe, A.L., Bown, P.R., Rawson, P.F., Gale, A., Gibbard, P., Gregory, F.J., Hounslow, M.W., Kerr, A.C., Pearson, P., Knox, R., Powel, J., Waters, C., Marshall, J., Oates, M., & Stone, P. (2011): Stratigraphy of the anthropocene. *Philos. Trans. R. Soc. A Math. Phys. Eng. Sci*, **369**, 1036–1055.